THE UNIVERSITY OF QUEENSLAND

Bachelor of Engineering Thesis

Corrosion of Ti biomaterials

Student Name: Jayde MCELLIGOTT

Course Code: MECH4500

Supervisor: Professor Andrej Atrens

Submission date: 28 October 2016

A thesis submitted in partial fulfilment of the requirements of the Bachelor of Engineering degree in Mechanical Engineering

UQ Engineering

Faculty of Engineering, Architecture and Information Technology

Abstract

The experimental investigation of corrosion stability of Ti-35.4Zr-28Nb in synthetic body fluid was conducted to aid in the development of a porous Ti alloy for use as a bone replacement material. The corrosion analysis was conducted using immersion testing for 28 days, Open Circuit Potential (OCP), Electrochemical Impedance Spectroscopy (EIS) and potentiodynamic polarisation curves. The corrosion performance of the Ti alloy was compared to that of commercial purity (CP Ti) Grade 2 under in-vitro testing conditions in:

1. Hanks' solution at 37 °C
2. 3.5% NaCl solution at 95 °C

Immersion testing results of both the materials showed negligible weight loss and low concentration of Ti, Zr and Nb, which indicates a low corrosion rate. In addition, the electrochemical testing indicated passivation behaviour which was further supported by the partial stabilisation of current density and overall low current densities (in the order of 10^{-6} A/cm^2). The OCP measurement also described a passivation behaviour with an increase in the corrosion potential and a stabilised curve over time.

Overall, from the experimental results, no significant evidence of crevice corrosion was observed under the testing conditions indicating that both CP Ti and the Ti alloy are not sensitive to crevice corrosion.

Acknowledgements

I take this opportunity to express gratitude to Professor Andrej Atrens for his advice and support throughout this year.

I also thank Dr Zhiming Shi and Mr Akif Soltan for sharing their wealth of knowledge with me. Thank you for spending the time to explain concepts and methods, and helping conduct the experiments.

Finally, I thank my family and friends for their love, encouragement and support throughout this journey.

Table of Contents

Abstract ii

Acknowledgements iii

List of Tables vi

List of Figures vii

Corrosion of Ti biomaterials 1

1. Introduction 1

1.1. Project Aims 2

1.2. Project Scope 2

2. Literature Review 3

2.1. Titanium 3

2.2. Overview of Titanium Corrosion 3

2.3. Crevice Corrosion Testing 4

2.4. Previous Work 5

2.5. Electrochemical Testing 6

3. Methodology 7

3.1. Immersion Testing 7

3.1.1. Sample Preparation 7

3.1.2. Weight Loss Measurements 7

3.1.3. Coupon Assembly 8

3.1.4. Hanks' solution 9

3.1.5. NaCl solution 10

3.1.6. Scanning Electron Microscopy (SEM) 11

3.2. Electrochemical Testing 11

3.2.1. Sample preparation 12

3.2.2. Hanks' solution 12

3.2.3. NaCl solution 13

4. Experimental Results 14

4.1. Immersion Testing 14

4.1.1. Surface Morphology 14

4.1.1.1. Hanks' Solution 14

4.1.1.2. NaCl Solution 15

4.1.2. Weight Loss Measurements 17

4.1.2.1. Hanks' Solution 17
4.1.2.2. NaCl solution 18
4.2. Surface composition 18
4.2.1.1. Hanks' solution 18
4.2.1.2. NaCl solution 19
4.2.2. Solution Analysis 20
4.3. Electrochemical Testing 20
4.3.1. Surface Area 20
4.3.2. Open Circuit Potential 20
4.3.2.1. Hanks' solution 20
4.3.2.2. NaCl solution 21
4.3.3. Electrochemical Impedance Spectroscopy 22
4.3.3.1. Hanks' solution 22
4.3.3.2. NaCl solution 25
4.3.4. Potentiodynamic Polarisation Curve 28
4.3.4.1. Hanks' solution 28
4.3.4.2. NaCl solution 29
5. Discussion 31
5.1. Immersion Testing 31
5.1.1. Surface Morphology 31
5.1.2. Weight Loss Measurements 31
5.1.3. Surface Composition 31
5.1.4. Solution Analysis 31
5.2. Electrochemical Testing 32
5.2.1. OCP 32
5.2.2. EIS 32
5.2.3. Potentiodynamic Polarisation Curve 32
5.3. Experimental Difficulties 33
6. Conclusion 35
7. References 36
8. Appendices 39
8.1. Appendix A 39

List of Tables

Table 1: Samples used in each coupon 14
Table 2: Weight loss measurements for CP Ti in Hanks' solution at 37 °C after 28 days 17
Table 3: Weight loss measurements for Ti alloy in Hanks' solution at 37 °C after 28 days 17
Table 4: Weight loss measurements for CP Ti in NaCl solution at 95 °C after 28 days 18
Table 5: Weight loss measurements for Ti alloy in NaCl solution at 95 °C after 28 days 18
Table 6: Solution analysis after immersion testing 20
Table 7: Surface area of samples used in the electrochemical tests 20
Table 8: Characteristics of the Bode plot in Hanks' solution at 37 °C 24
Table 9: Characteristics of the Nyquist plot in Hanks' solution at 37 °C 25
Table 10: Characteristics of the Bode plot in 3.5% NaCl solution at 23 °C 26
Table 11: Characteristics of the Nyquist plot in 3.5% NaCl solution at 23 °C 28
Table 12: Characteristics of the polarisation curves in Hanks' solution at 37 °C 29
Table 13: Characteristics of the polarisation curves in 3.5% NaCl solution at 37 °C 30

List of Figures

Figure 1: Crevice corrosion mechanism (Temenoff and Mikos, 2008)..... 4
Figure 2: (a) Schematic of coupon assembly, (b) Schematic of Ti plate 8
Figure 3: (a) CP Ti coupon assembly, (b) Ti35Zr28Nb alloy coupon assembly 9
Figure 4: Water bath set up showing one coupon assembly 10
Figure 5: NaCl solution immersion testing set up showing one coupon assembly..... 11
Figure 6: Electrochemical testing set up 12
Figure 7: CP Ti sample 4 after 28 days in Hanks' solution at 37 °C 14
Figure 8: TiZrNb sample 4 after 28 days in Hanks' solution at 37 °C 15
Figure 9: CP Ti sample 2 after 28 days in 3.5% NaCl solution at 95 °C 16
Figure 10: TiZrNb sample 2 after 28 days in 3.5% NaCl solution at 95 °C 16
Figure 11: EDX spectra of TiZrNb sample 4 after 28 days in Hanks' solution at 37 °C 19
Figure 12: EDX spectra of TiZrNb sample 1 after 28 days in 3.5% NaCl solution at 95 °C 19
Figure 13: OCP comparison of all samples in Hanks' solution at 37 °C 21
Figure 14: OCP comparison of all samples in 3.5% NaCl solution at 23 °C 22
Figure 15: Bode plot comparison of all samples in Hanks' solution at 37 °C 23
Figure 16: Phase plot comparison of all samples in Hanks' solution at 37 °C..... 24
Figure 17: Nyquist plot comparison of all samples in Hanks' solution at 37°C 25
Figure 18: Bode plot comparison of all samples in 3.5% NaCl solution at 23 °C 26
Figure 19: Phase plot comparison of all samples in 3.5% NaCl solution at 23 °C..... 27
Figure 20: Nyquist plot comparison of all samples in 3.5% NaCl solution at 23 °C 27
Figure 21: Polarisation curve comparison of all samples in Hanks' solution at 37 °C 28
Figure 22: Polarisation curve comparison of all samples in 3.5% NaCl solution at 23 °C 30

Corrosion of Ti biomaterials

1. Introduction

A biomaterial, as defined by the National Institutes of Health (NIH), is "any substance (other than a drug) or combination of substances, synthetic or natural in origin, which can be used for any period of time, as a whole or as a part of a system which treats, augments, or replaces any tissue, organ, or function of the body" (Birla, 2014). Biomaterials are used for orthopedic implants required for congenital defects, traffic accidents, or sports injuries, as well as bone tissue diseases associated with aging (Ozan et al., 2015). According to the World Health Organization, in 2030 there will be 1.4 billion people aged 60 years and older, which equates to a 56% increase from 2015. This increases the need for further research into materials suitable for biomedical applications.

Materials suitable for these applications must possess properties such as non-toxicity, corrosion resistance, fatigue resistance, and biocompatibility (Watanabe et al., 2015). There are four general categories for biomaterials: metals, polymers, ceramics and composites (Binyamin et al., 2006). Of these materials, metals are most commonly used, in particular titanium and its alloys. This is due to its biocompatibility, high corrosion resistance, high strength-to-weight ratio, and reasonable formability (Assis et al., 2006, Martins et al., 2008). Furthermore, titanium promotes osseointegration, which allows for bone ingrowth or the fixing of an implant to a patient's bone structure (Cremasco et al., 2008). Current applications for titanium and titanium alloys include bone and joint replacement, dental implants, fracture fixation and stents (Davis, 2003).

However, titanium has a higher elastic modulus than bone. This is undesirable as this may result in stress shielding and implant loosening (Fojt et al., 2013). This highlights the need for alloys and porous materials.

Elements such as Nb, Ta, Zr, Mo and Sn are considered to be safe Ti alloying elements. They are non-toxic and non-allergic, and are excellent beta phase stabilisers (Cremasco

et al., 2008). However, the use of Mo is still considered to be controversial (Nnamchi et al., 2016).

1.1.Project Aims

The aim of this research project is to assess the corrosion stability of Ti-35.4Zr-28Nb in a synthetic body fluid. This research will aid in the development of a porous Ti alloy for use as a bone replacement material.

1.2.Project Scope

The corrosion performance of the Ti alloy will be compared to that of commercial purity (CP Ti) Grade 2 under in-vitro testing conditions in the following solutions:

1. Hanks' solution at 37 °C
2. 3.5% NaCl solution at 95 °C

The experimental investigation study corrosion of the Ti alloy using the following methods:

1. Investigation of crevice corrosion during immersion testing for 28 days.
2. Investigation of the corrosion electrochemistry using measurements of the Open Circuit Potential (OCP), Electrochemical Impedance Spectroscopy (EIS) and potentiodynamic polarisation curves.

2. Literature Review

2.1.Titanium

Titanium alloys, particularly those that are free of vanadium (V) and aluminum (Al) as opposed to the common aerospace grade Ti-6Al-4V alloy, have received high interest as titanium is considered one of the most important biocompatible metals (Bansiddhi and Dunand, 2014). Biocompatibility is important as it is the biological acceptance of the implant by the body. The absence of V and Al from the Ti alloy is critical as they are elements that exhibit high cytotoxicity and negative tissue response in vivo conditions. Possible impacts include induced senile dementia, neurological disorders and allergic reactions (Martins et al., 2008).

Consequently, recent research has focused on β-titanium alloys due to increased biocompatibility and decreased elastic modulus compared to α-phase. Similar elastic modulus of the bone and the implant promotes a load sharing between the implant and natural bone and minimises stress shielding (Martins et al., 2008). The beta phase is present at high temperatures, so in order to stabilise it at lower temperatures and obtain an elastic modulus closer to that of the natural bone, the aforementioned beta phase stabilisers are required (Nnamchi et al., 2016).

2.2.Overview of Titanium Corrosion

Jones (1996) describes corrosion as the "destructive result of chemical interactions between a material and its environment". Corrosion can have detrimental effects including the loss of product, product efficiency, and contamination, or more significantly, the loss of human life (Jones, 1996).

The excellent corrosion properties of Ti are due to the formation of oxide film on the surface of titanium (Jones, 1996). If passivity breakdown of Ti does occur, as is most likely in bio-applications, the most likely situation is in the form of crevice corrosion (Cramer et al., 2003).

Passive metals are particularly susceptible to crevice corrosion in environments containing chloride (Cheng et al., 2007).

2.3.Crevice Corrosion Testing

Of particular importance to biomaterials is crevice corrosion. Crevice corrosion occurs in areas where narrow, deep cracks are present. An example is the point of contact between a screw and plate of a bone fixation device (Temenoff and Mikos, 2008).

As discussed by Temenoff and Mikos (2008), crevice corrosion is initiated when oxygen is depleted in a crevice; the crevice acts as the anode whilst the remaining metal is the cathode. This limits the supply of oxygen from outside the crevice via diffusion only (Cheng et al., 2007).

Figure 1 shows the theoretical mechanism of crevice corrosion. The concentration of metal ions (M^{n+}) in the crevice solution increases due to anodic dissolution. These ions then attract chloride ions (Cl^-) from the bulk of the solution in order to maintain electrical neutrality. Unstable metallic chlorides are then formed, which then hydrolyse to produce H^+ ions. This results in a lower pH of the crevice solution. The reduction in pH further dissolution of the metal, thus attracting more chloride ions, and further lowering the pH. This process is considered to be autocatalytic. The crevice solution becomes increasingly aggressive due to the increased concentration of Cl^- and H^+(Cheng et al., 2007). The overall reaction can be written as:

$$MCl_n + nH_2O \rightarrow M(OH)_n + nH^+Cl^-$$

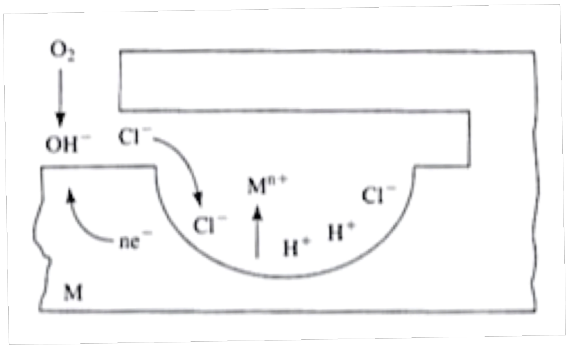

Figure 1: Crevice corrosion mechanism (Temenoff and Mikos, 2008)

The pH of normal human blood is 7.4 ± 0.05; values outside of the range 7-7.7 are deemed terminal (Zainal Abidin et al., 2011). Hence, it is important to limit any potential corrosion from biomaterials which fluctuates the pH of the blood.

2.4.Previous Work

Previous research on biocompatible Ti alloys has focused on a variety of factors. In their research, Nnamchi et al. (2016) performed potentiodynamic polarisation tests on Ti-Mo-Nb-Zr alloy. Similarly, Lopes et al. (2016) used OCP and potentiodynamic polarisation curves to test Ti-Nb-Fe.

Other research have used similar alloys but different testing conditions that did not simulate the body conditions. For example, Martins et al. (2008) and Cremasco et al. (2008) tested Ti-30Nb-Zr and Ti-35Nb respectively using electrochemical testing in 0.9% NaCl solution at 25°C.

There have also been other research that used similar alloys but with different testing methods. Fojt et al. (2013) tested Ti39Nb for crevice corrosion but they concluded that "given the assumption that the corrosion process was localised in the pores, no artificial crevice was formed on the specimens, in contrast to the standardized procedure." Cheng et al. (2007) also tested crevice corrosion of NiTi using compartmentalised cell.

Niemeyer et al. (2009) and Assis et al. (2006) both tested Ti-13Nb-13Zr but didn't test specifically for crevice corrosion behaviour. Niemeyer et al. (2009) tests for corrosion behaviour of sample "with oxygen loads by doping the samples with two quantities of interstitial oxygen in a PBS solution". Similarly Xu et al. (2015) used potentiodynamic polarisation curves to examine the corrosion of Ti-Nb-Ta-Zr-Fe, however crevice corrosion was not the main focus.

Past works also included studies of crevice corrosion, but with different material. For example, Chenghao et al. (2015) tested CP Ti, Ti-6Al-4V and Ti-Ni Shape Memory Alloy for crevice corrosion.

There was also one study that used the exact alloy but the investigation focused on mechanical properties rather than corrosion. Ozan et al. (2015) tested Ti-34Nb-25Zr, Ti-30Nb-32Zr, Ti-28Nb-35.4Zr and Ti-24.8Nb-40.72Zr for "effects of alloying element on their microstructures, mechanical properties and cytocompatibilities."

2.5.Electrochemical Testing

Polarisation curves are plots of current versus electrode potential. The corrosion rate, i_{corr}, can be found at E_{corr} via extrapolation of the Tafel region (Jones, 1996).

3. Methodology

Two different testing methods were used to study the corrosion of Ti-35.4Zr-28Nb - immersion testing and electrochemical testing. CP Ti was tested as a control material.

3.1. Immersion Testing

Immersion testing was conducted using Hanks' solution and 3.5% NaCl solution. The sample preparation in both cases was the same. Weight loss measurements of the samples were taken before immersion tests and the coupons were assembled following this. Another set of weight loss measurements were conducted after the immersion tests.

3.1.1. Sample Preparation

1. CP Ti samples were cut to size (10 mm x 10 mm) using a Struers Discotom-6 cutting machine. The Ti alloy samples were already available as per the required size (10 mm x 10 mm).
2. All samples were ground sequentially using Struers Tegraforce-5 orbital machine with a 320-grit followed by 600-, 1200- and 4000-grit silicon carbide abrasive paper. The samples were rinsed with ethanol and dried with compressed air between each grinding step.
3. The samples were then polished using Struers Oxide Polishing Suspension with hydrogen peroxide (OP-S + 20% H_2O_2) to 0.5 micron.
4. After the polishing, the samples were placed in a beaker of ethanol and ultrasonically cleaned for 3 – 4 minutes, and dried with compressed air.
5. After the cleaning, all samples were placed in a zip lock bags and kept in a desiccator.

3.1.2. Weight Loss Measurements

Prior to the weight loss measurements, all samples were photographed using an optical microscope. The samples were then weighed using an analytical balance and the sample coupons assembled. After immersion testing had concluded, each sample was re-photographed and re-weighed. The reduction in weight was then calculated.

3.1.3. Coupon Assembly

Once all samples had been prepared, photographed and weighed, the coupons were assembled. Each coupon contained 3 Ti samples and 4 polytetrafluoroethylene (PTFE) washers to simulate a crevice (see Figure 2). The following steps were used to assemble each coupon:

1. A stack of alternating washers and samples was constructed.
2. A Ti plate was placed at each end of the stack.
3. Four Ti bolts were then inserted through each hole on the plate (see Figure 2).
4. A nut was threaded onto the end of each bolt and tightened with a spanner until evenly tight.

Images of the assembled coupons are shown in Figure 3.

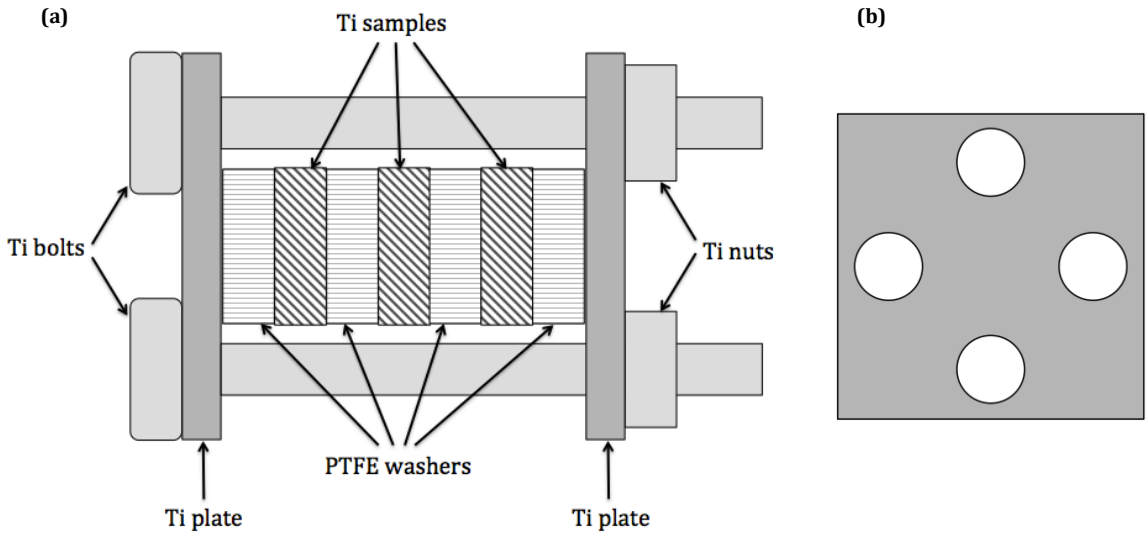

Figure 2: (a) Schematic of coupon assembly, (b) Schematic of Ti plate

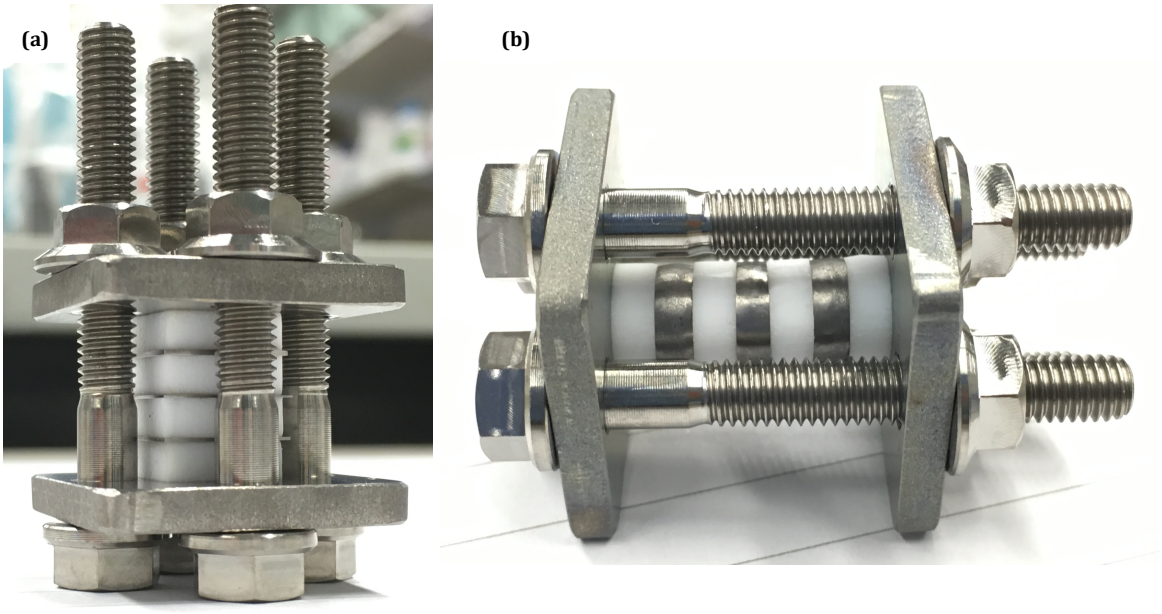

Figure 3: (a) CP Ti coupon assembly, (b) Ti35Zr28Nb alloy coupon assembly

3.1.4. Hanks' solution

After all the coupons were assembled, immersion testing commenced in Hanks' solution using the following steps:

1. 1 litre of Hanks' Balanced Salts was prepared with the addition of 0.35 g/L sodium bicarbonate, as per instructions (see Appendix A).
2. Two CP Ti coupons were placed in one beaker and two Ti alloy coupons were placed in another beaker.
3. 500 ml of Hanks' solution was added to each beaker.
4. The beakers were covered in gladwrap to minimise evaporation effects.
5. The beakers were then placed in a water bath at 37 °C (see Figure 4).
6. After 28 days the beakers were removed.
7. The coupons were removed from the Hanks' solution, rinsed with distilled water and dried with air. The coupons were placed in a zip lock bag and kept in the desiccator.
8. After several days of drying, the coupons were disassembled and the samples were re-weighed and photographed.

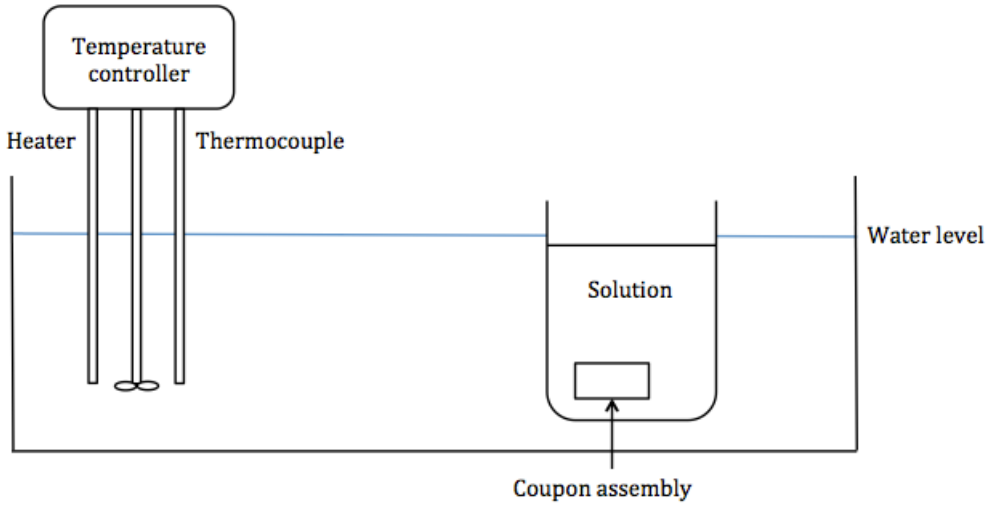

Figure 4: Water bath set up showing one coupon assembly

3.1.5. NaCl solution

The immersions tests in NaCl solution were conducted similarly to the tests in Hanks' solution (see Figure 5). The following steps were followed:

1. 1 litre of 3.5% NaCl solution was prepared using 35 g of NaCl and 1 L distilled water.
2. Two CP Ti coupons were placed in one flask and two Ti alloy coupons were placed in another flask.
3. 600 ml of NaCl solution was added to each flask.
4. Each flask was placed on a separate hotplate.
5. The condenser was then inserted into mouth of the flask using a B55 socket adaptor.
6. Hosing was connected between the condensers and tap. The water was then slowly turned on for the cooling system to function.
7. A thermocouple sensor connected to the hot plate was inserted in the flask to measure and control the solution temperature to 95 °C.
8. After 28 days the hot plate was turned off. When the flask had cooled sufficiently it was removed from the hot plate.
9. The coupons were removed from the flask, rinsed with distilled water and dried with air. The coupons were placed in a zip lock bag and kept in the desiccator.
10. After several days of drying, the coupons were disassembled and the samples were re-weighed and photographed.

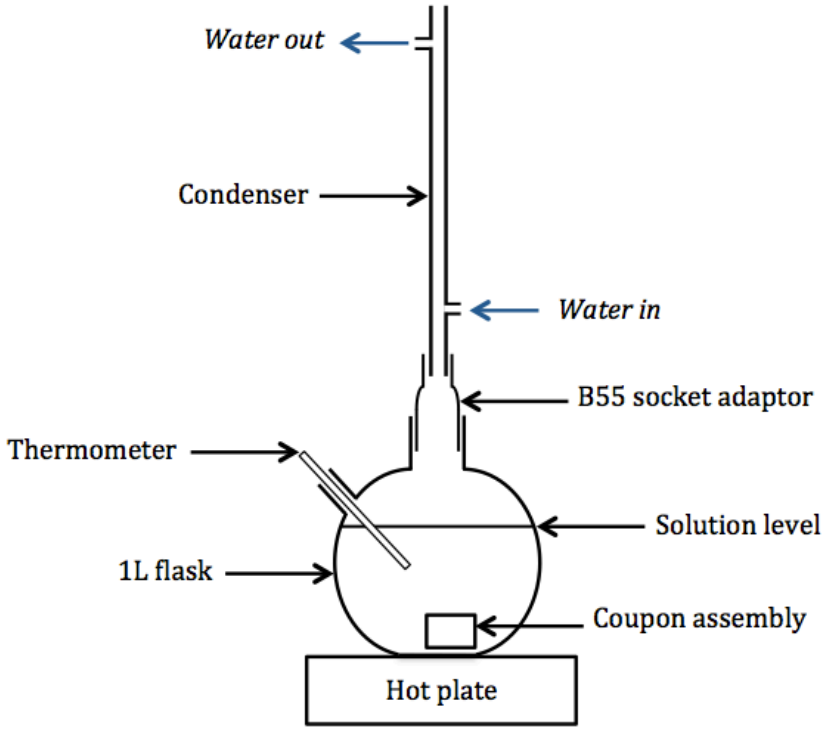

Figure 5: NaCl solution immersion testing set up showing one coupon assembly

3.1.6. Scanning Electron Microscopy (SEM)

The surface morphology was conducted using a JEOL JSM-6460 Scanning Electron Microscope with Energy-Dispersive X-ray Spectroscopy (EDX) microanalysis capabilities.

3.2. Electrochemical Testing

Electrochemical tests were conducted in both Hanks' solution and NaCl solution using a PARSTAT 2263 Advanced Electrochemical System. The software used was Princeton Applied Research Electrochemistry PowerSuite. A silver/silver chloride electrode saturated with potassium chloride (Ag/AgCl Sat. KCl) was used as a reference electrode.

Before testing could commence, the samples were prepared as follow.

3.2.1. Sample preparation

The samples were prepared in the following way:

1. The samples were ground sequentially using 320-, 600-, 1200-, 4000-grit silicon carbide abrasive paper, as per the immersion testing. The samples were rinsed with ethanol and dried with compressed air between each step.
2. A copper wire was laser welded to each sample.
3. The samples were then set in an epoxy resin, with the copper connection covered by epoxy, and exposing a surface area of approximately 1 cm^2.
4. Each sample was numbered using a Dremyl for identification purposes.
5. All samples were repolished using 4000-grit silicon carbide to remove any epoxy resin on the outer surface.
6. The surface area of each sample was measured and recorded.

3.2.2. Hanks' solution

The testing was setup using the following steps:

1. A beaker was filled with 500 ml of Hanks' solution.
2. The beaker was placed in a water bath at 37 °C.
3. The beaker was left for 30 minutes to ensure the solution in the beaker has equilibrated to the temperature of the bath. The sample was then clamped into place and lowered into the solution.
4. The counter electrode was placed on the side of beaker. The sample (working electrode) and the reference electrode were placed in close proximity (see Figure 6).

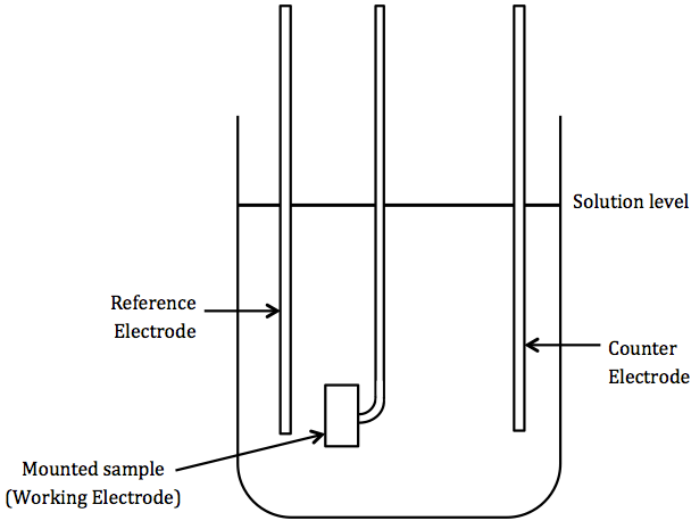

Figure 6: Electrochemical testing set up

Open Circuit Potential (OCP)

The corrosion potential (E_{corr}) was monitored over a period of 7200 seconds, with data being recorded every 2 seconds.

Electrochemical Impedance Spectroscopy (EIS)

Once the OCP had finished, the EIS was conducted. The electrochemical impedance (Z) was measured over a frequency range from 100 kHz to 10 mHz, using an AC amplitude of 10 mV. A total of 40 data points were collected.

Potentiodynamic polarisation curve

The final electrochemical test was the polarisation curve. Scans were carried out at a scan rate of 0.1660 mV/s in the range from -0.2500 to 3.0000 volts.

At the completion of polarisation curve, the sample was removed from the solution and rinsed with distilled water, dried with compressed air and placed in zip locked bag.

3.2.3. NaCl solution

Before the samples could be tested in NaCl solution they were ground using 4000-grit silicon carbide to remove any passive film that could have formed on the sample surface. The sample was then rinsed with ethanol and dried with compressed air. The test was then set up as per the methodology in section 3.2.2, however, substituting 500 ml of 3.5% NaCl solution at room temperature (23 °C) for the Hanks' solution.

4. Experimental Results

The experimental results for the immersion and electrochemical testing can be found in sections 4.1 and 4.3 respectively.

4.1.Immersion Testing

Table 1 shows the sample designation for immersion testing in both the Hanks' and NaCl solutions.

Table 1: Samples used in each coupon

Coupon	Material	Samples
1	Ti alloy	1, 2, 3
2	Ti alloy	4, 5, 6
3	CP Ti	1, 2, 3
4	CP Ti	4, 5, 6

4.1.1. Surface Morphology

4.1.1.1. Hanks' Solution

Figure 7 shows the surface morphology as observed by SEM of a CP Ti sample immersed in Hanks' solution for 28 days. The image shows no evidence of pitting or crevice corrosion. However, potential filiform corrosion can be seen.

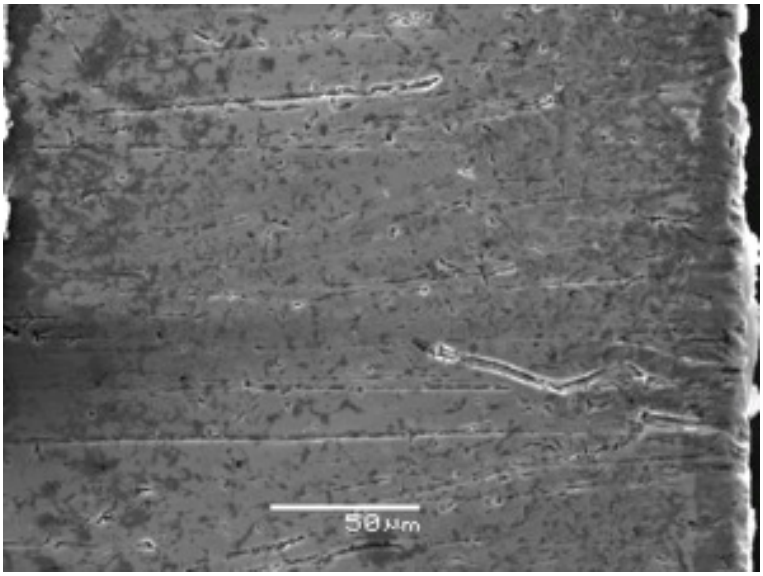

Figure 7: CP Ti sample 4 after 28 days in Hanks' solution at 37 °C

Figure 8 shows similar morphology for the TiZrNb alloy after immersion in Hanks' solution for 28 days. The formation of a surface layer can be seen on the outer edge of the sample. This is analysed further in section 4.2.1.1 There is no evidence of crevice corrosion.

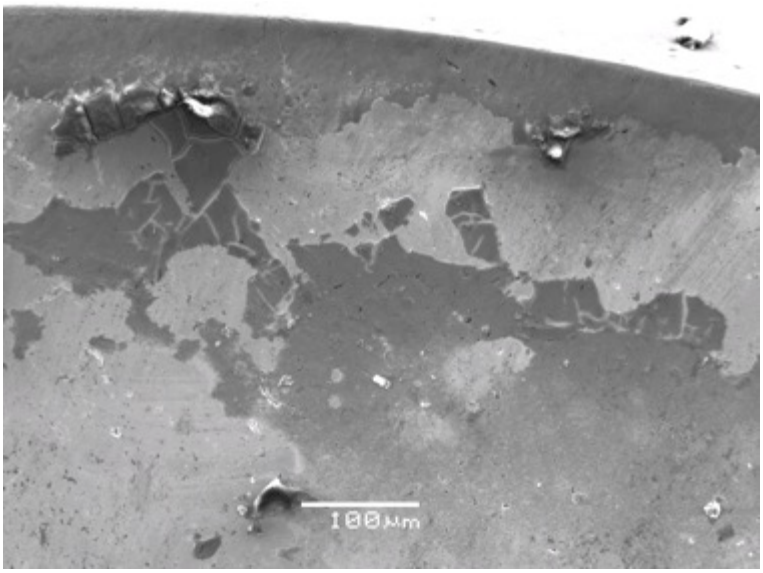

Figure 8: TiZrNb sample 4 after 28 days in Hanks' solution at 37 °C

4.1.1.2. NaCl Solution

Figure 9 show the corrosion morphology of typical CP Ti samples immersed in 3.5% NaCl solution for 28 days. An image of a typical TiZrNb sample is shown in Figure 10.

CP Ti shows a predominantly uniform surface and there is no evidence of crevice corrosion as illustrated in Figure 9.

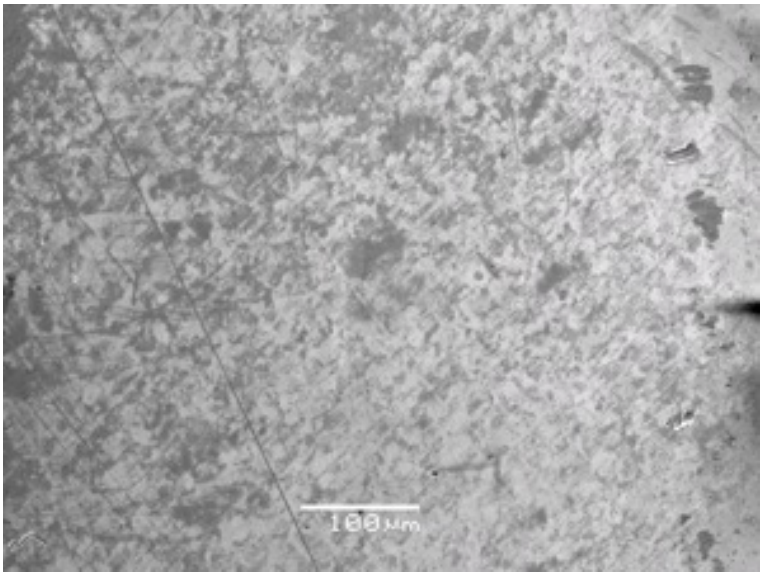

Figure 9: CP Ti sample 2 after 28 days in 3.5% NaCl solution at 95 °C

The TiZrNb sample shows two distinct sections. The outer area of the sample was in contact with both the washer and NaCl solution. The inner section was in contact with the washer only. A number of scratches can be seen along the outer edge of the sample from the polishing step. There is no evidence of crevice corrosion.

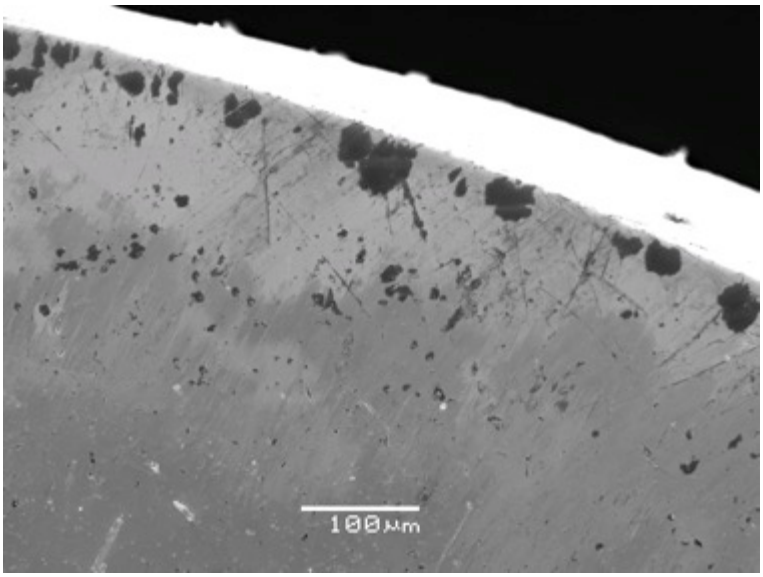

Figure 10: TiZrNb sample 2 after 28 days in 3.5% NaCl solution at 95 °C

4.1.2. Weight Loss Measurements

Each sample was weighed before and after the immersion testing. The change in weight has been calculated in mass (g). The change in weight was calculated using the following equation:

$$\Delta m\ (g) = weight_{before} - weight_{after}$$

4.1.2.1. Hanks' Solution

Table 2 and Table 3 show the weight loss measurements for CP Ti and the Ti alloy in Hanks' solution at 37 °C after 28 days.

Table 2: Weight loss measurements for CP Ti in Hanks' solution at 37 °C after 28 days

Sample	Weight (g)		Δm (g)
	Before	After	
1	0.2973	0.2970	0.0003
2	0.3027	0.3027	0.0000
3	0.3068	0.3068	0.0000
4	0.2977	0.2976	0.0001
5	0.3165	0.3163	0.0002
6	0.2983	0.2982	0.0001

Table 3: Weight loss measurements for Ti alloy in Hanks' solution at 37 °C after 28 days

Sample	Weight (g)		Δm (g)
	Before	After	
1	0.8013	0.8011	0.0002
2	0.8116	0.8113	0.0003
3	0.8053	0.8050	0.0003
4	0.7903	0.7903	0.0000
5	0.8013	0.8012	0.0001
6	0.7308	0.7308	0.0000

4.1.2.2. NaCl solution

Table 5 show the weight loss measurements for CP Ti and the Ti alloy in NaCl solution at 95 °C after 28 days.

Table 4: Weight loss measurements for CP Ti in NaCl solution at 95 °C after 28 days

Sample	Weight (g)		Δm (g)
	Before	After	
1	0.1415	0.1414	0.0001
2	0.1348	0.1346	0.0002
3	0.2351	0.2350	0.0001
4	0.1250	0.1245	0.0005
5	0.0719	0.0719	0.0000
6	0.1209	0.1209	0.0000

Table 5: Weight loss measurements for Ti alloy in NaCl solution at 95 °C after 28 days

Sample	Weight (g)		Δm (g)
	Before	After	
1	0.7878	0.7877	0.0001
2	0.6664	0.6661	0.0003
3	0.7724	0.7724	0.0000
4	0.8077	0.8077	0.0000
5	0.8109	0.8108	0.0001
6	0.7184	0.7182	0.0002

4.2. Surface composition

4.2.1.1. Hanks' solution

Figure 11 shows the surface composition of a typical TiZrNb sample immersed in Hanks' solution for 28 days. Traces of calcium (Ca), phosphorus (P) and oxygen (O) are present.

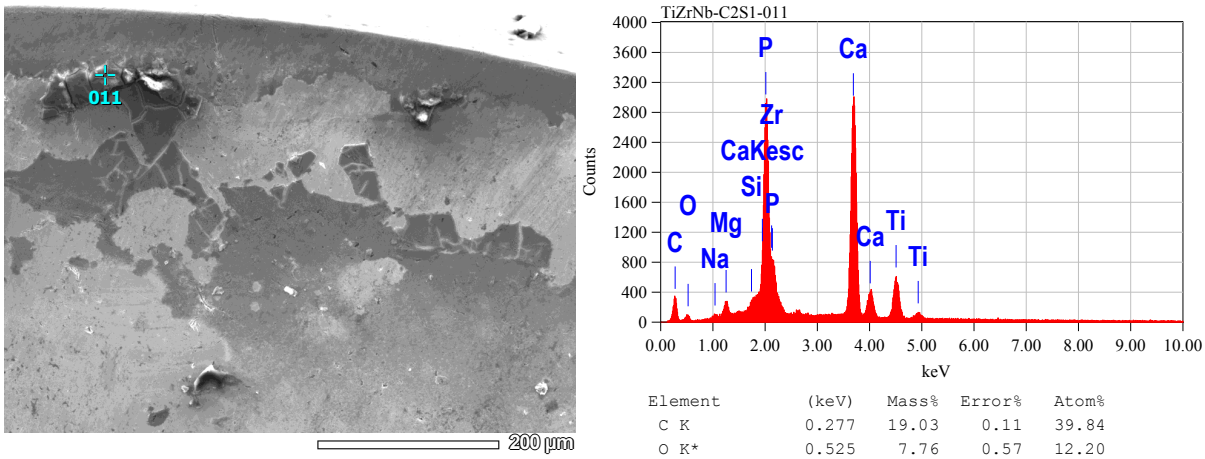

Element	(keV)	Mass%	Error%	Atom%
C K	0.277	19.03	0.11	39.84
O K*	0.525	7.76	0.57	12.20
Na K*	1.041	0.58	0.10	0.63
Mg K*	1.253	1.60	0.08	1.66
Si K	1.739	0.27	0.06	0.24
P K	2.013	19.83	0.07	16.10
Ca K	3.690	35.82	0.10	22.48
Ti K	4.508	10.79	0.14	5.66
Zr L	2.042	4.32	0.19	1.19
Total		100.00		100.00

Figure 11: EDX spectra of TiZrNb sample 4 after 28 days in Hanks' solution at 37 °C

4.2.1.2. NaCl solution

Figure 12 shows the surface composition of a typical TiZrNb sample immersed in 3.5% NaCl solution for 28 days. The presence of oxygen suggests the formation of an oxide layer. A slight decrease in both Zr and Nb contents is also observed, when compared to the original composition.

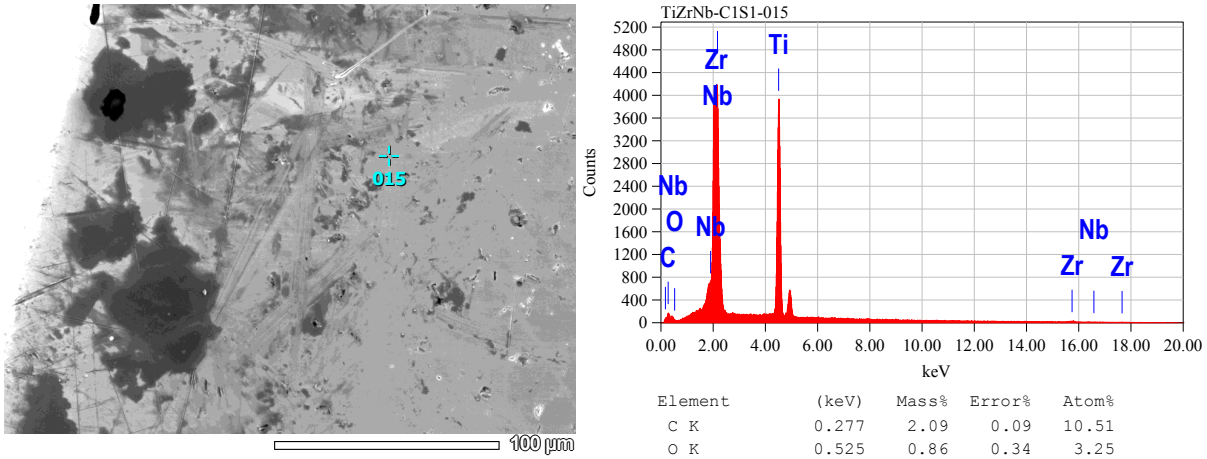

Element	(keV)	Mass%	Error%	Atom%
C K	0.277	2.09	0.09	10.51
O K	0.525	0.86	0.34	3.25
Ti K	4.508	37.29	0.09	47.00
Zr L	2.042	33.79	0.14	22.37
Nb L	2.166	25.96	0.13	16.87
Total		100.00		100.00

Figure 12: EDX spectra of TiZrNb sample 1 after 28 days in 3.5% NaCl solution at 95 °C

4.2.2. Solution Analysis

After each immersion test the solution was analysed for the concentration of Ti, Zr and Nb. The results are shown in Table 6.

Table 6: Solution analysis after immersion testing

Solution	Material	Solution concentration (mg/L)		
		Ti	Zr	Nb
Hanks' solution	CP Ti	0.001	-	-
	TiZrNb	0.002	0.001	0.016
3.5% NaCl solution	CP Ti	0.002	-	-
	TiZrNb	0.003	0.006	0.016

4.3.Electrochemical Testing

4.3.1. Surface Area

Table 7 presents the surface area of each sample.

Table 7: Surface area of samples used in the electrochemical tests

Material	Sample	Dimensions (mm)	Surface area (cm^2)
Ti alloy	1	Diam = 8mm	0.50
	2	Diam = 8mm	0.50
CP Ti	1	10.3 x 11.3	1.16
	2	10.5 x 13.3	1.40
	3	11.4 x 10.7	1.21

4.3.2. Open Circuit Potential

4.3.2.1. Hanks' solution

Figure 13 shows a comparison of OCP results for all CP Ti and Ti alloy samples in Hanks' solution at 37 °C. The corrosion potential is seen to increase quickly towards more positive potentials during the first hour (3600s). After that, the corrosion potential changes more slowly until it reaches a relatively stable level. This is observed for all samples.

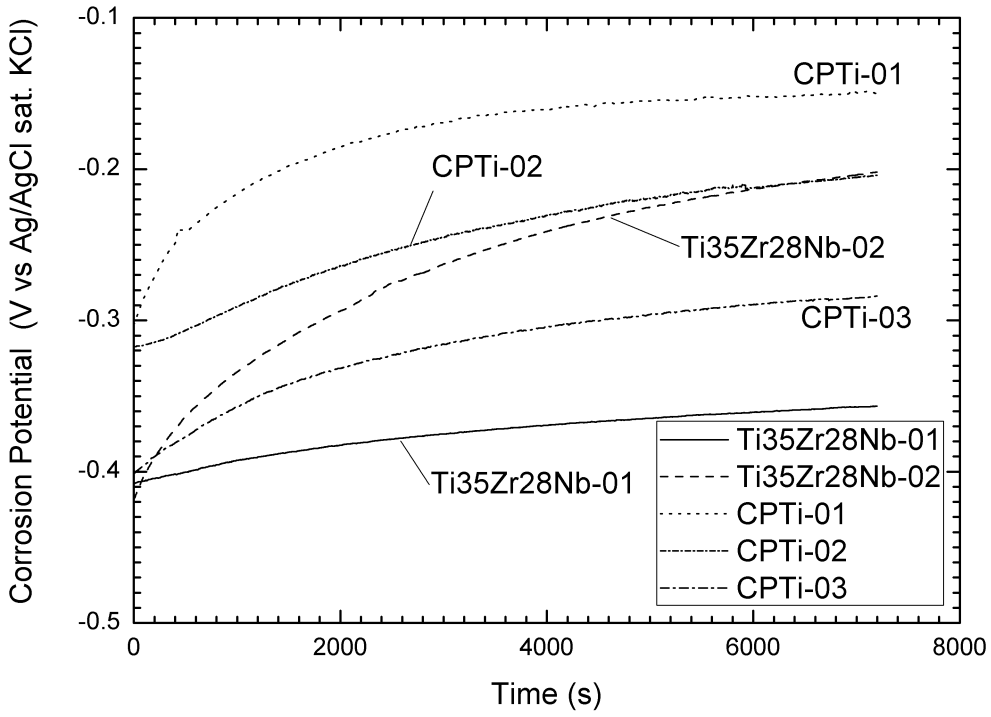

Figure 13: OCP comparison of all samples in Hanks' solution at 37 °C

4.3.2.2. NaCl solution

Figure 14 shows a comparison of OCP results for all CP Ti and the Ti alloy in 3.5% NaCl solution at room temperature (23 °C). The corrosion potential of Ti35Zr28Nb and CPTi-01 samples remain relatively stable for the duration of immersion. The corrosion potential of CPTi-02 increases quickly towards a more positive potential before it begins to stabilise, as illustrated in Figure 13.

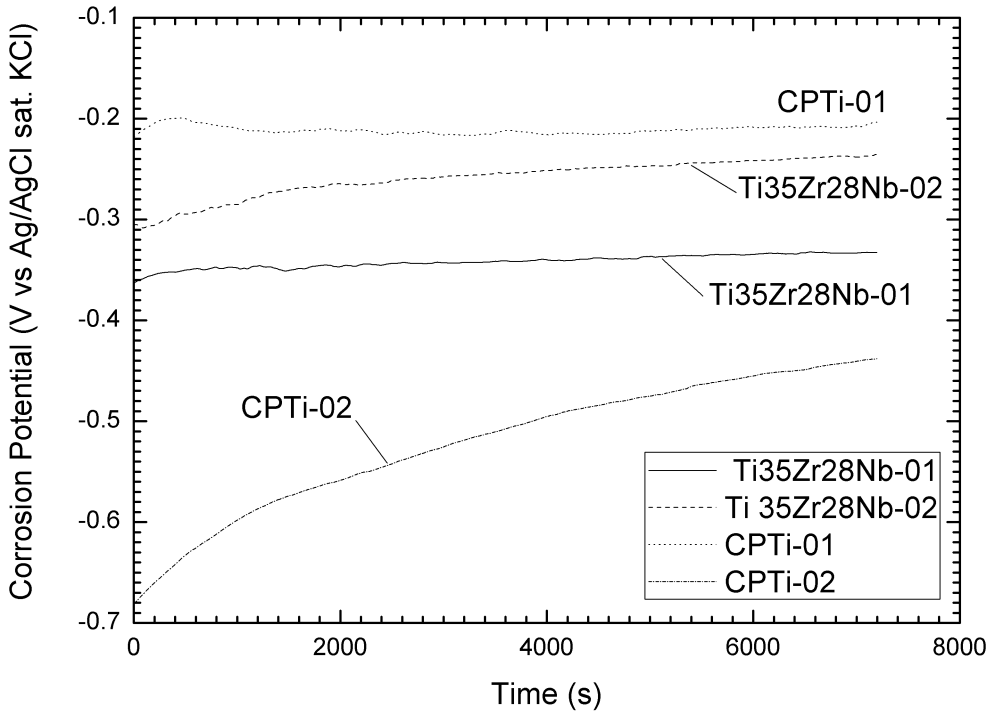

Figure 14: OCP comparison of all samples in 3.5% NaCl solution at 23 °C

4.3.3. Electrochemical Impedance Spectroscopy

EIS results include the bode, the phase and Nyquist plots. A bode plot graphs impedance (Z) versus frequency, while the phase plot shows the phase of impedance versus frequency. The Nyquist plot is the real versus imaginary part of the impedance.

4.3.3.1. Hanks' solution

The bode, phase and Nyquist plots comparing all samples in Hanks' solution at 37 °C are presented in Figure 14, Figure 16 and Figure 17 respectively.

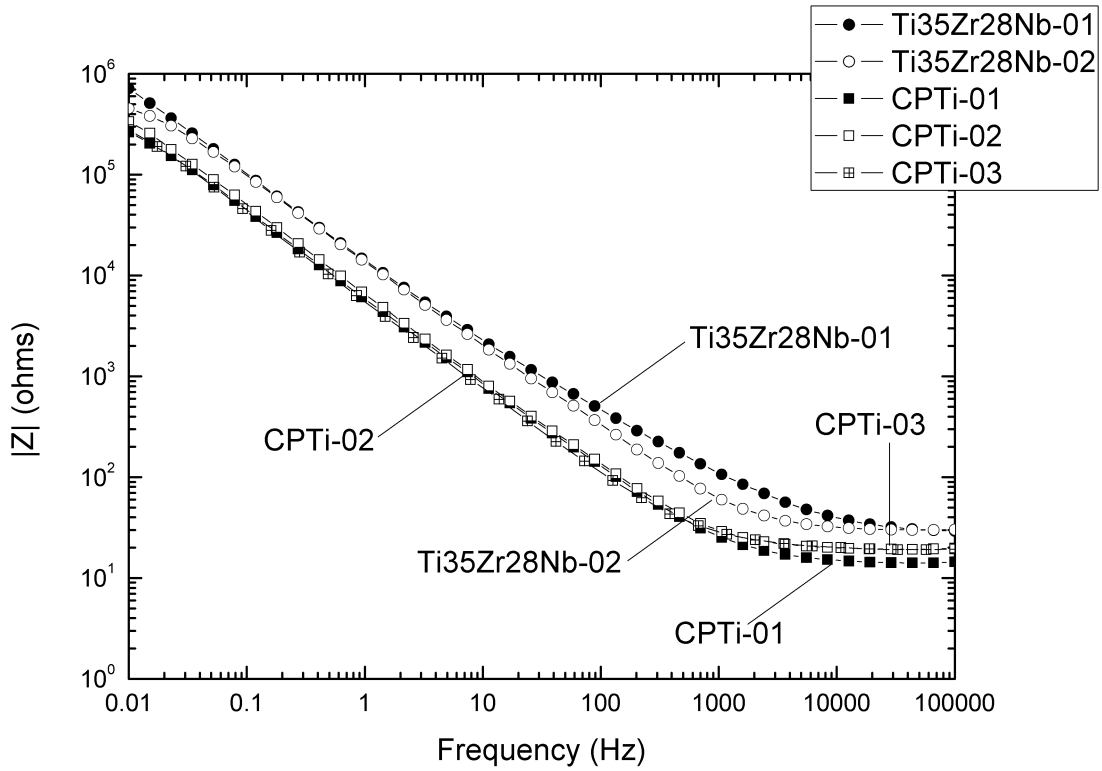

Figure 15 shows high modulus of impedance (Z) at low frequencies for all samples in Hanks' solution at 37 °C. This is also shown in Table 8.

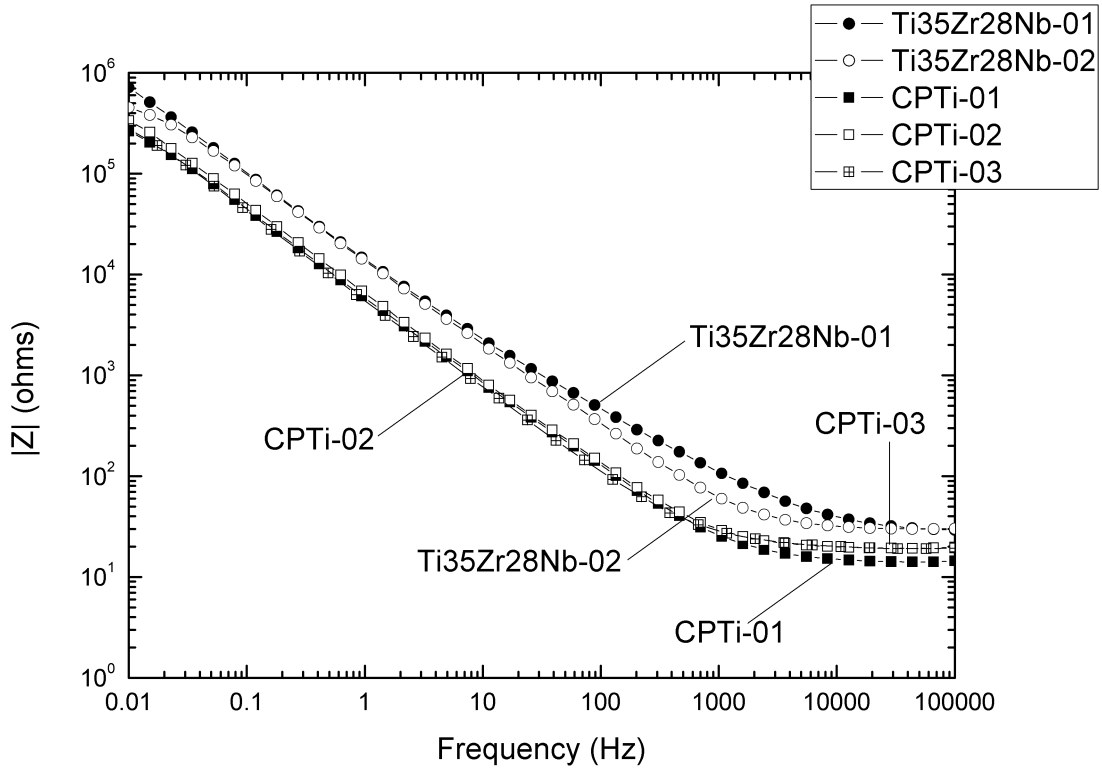

Figure 15: Bode plot comparison of all samples in Hanks' solution at 37 °C

Table 8: Characteristics of the Bode plot in Hanks' solution at 37 °C

Material	Sample	|Z| (kΩ)
CP Ti	1	264
	2	334
	3	280
Ti alloy	1	714
	2	452

Figure 16 shows the phase angle approaching 90° for medium to low frequencies. This is seen for all samples in Hanks' solution at 37 °C.

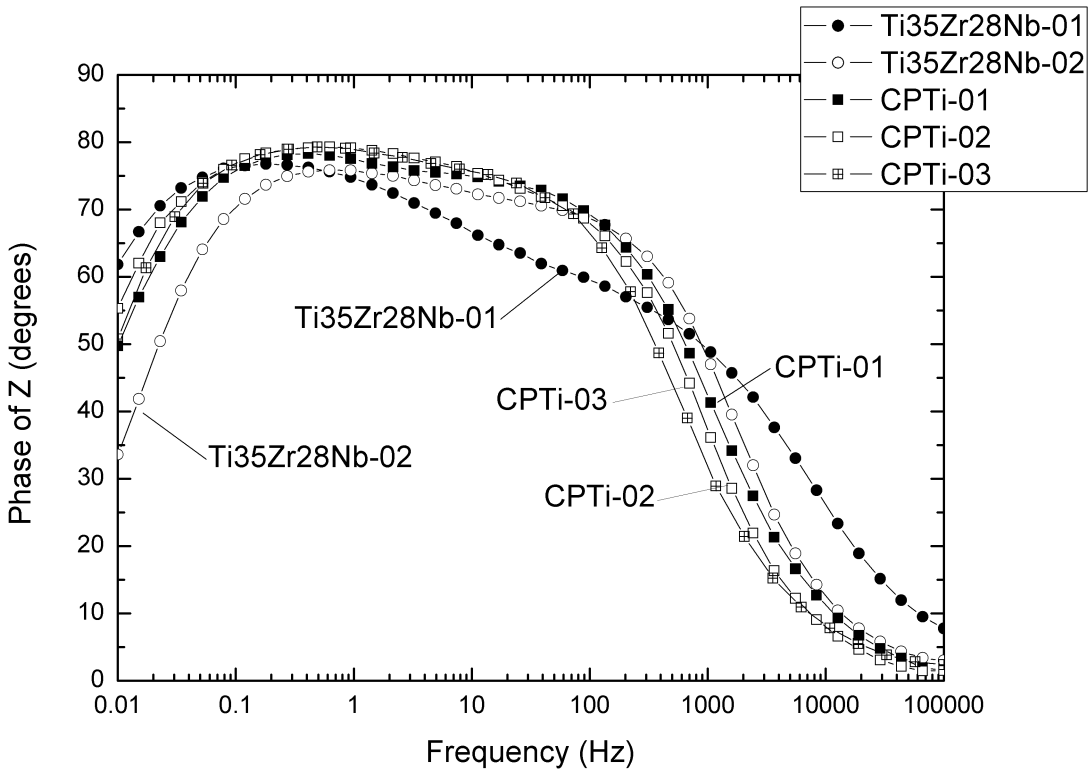

Figure 16: Phase plot comparison of all samples in Hanks' solution at 37 °C

Figure 17 shows the capacitance arcs of all samples in Hanks' solution at 37 °C. The estimated arc diameters are shown in Table 9.

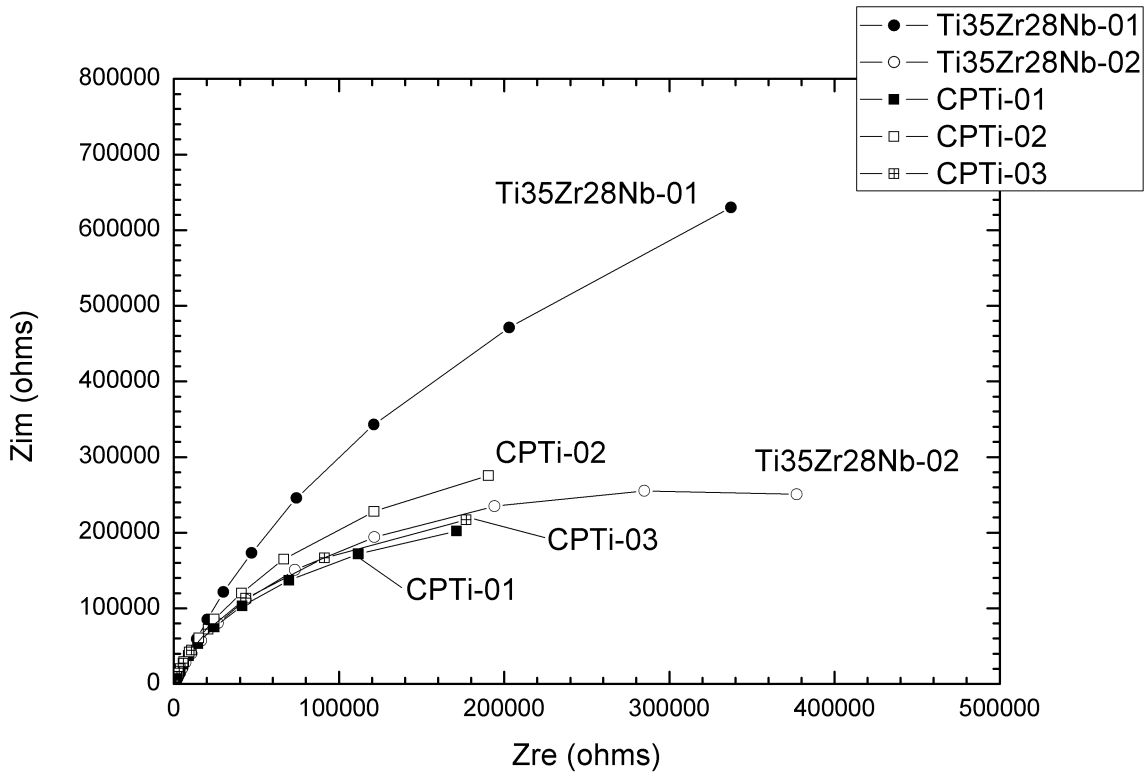

Figure 17: Nyquist plot comparison of all samples in Hanks' solution at 37°C

Table 9: Characteristics of the Nyquist plot in Hanks' solution at 37 °C

Material	Sample	Diameter (kΩ)
CP Ti	1	507
	2	753
	3	538
Ti alloy	1	2350
	2	630

4.3.3.2. NaCl solution

The bode, phase and Nyquist plots comparing all samples in 3.5% NaCl solution at room temperature (23 °C) are presented in Figure 18, Figure 19 and Figure 20 respectively.

Figure 18 shows high modulus of impedance (Z) at low frequencies for all samples in NaCl solution at 23 °C. This is also shown in Table 10.

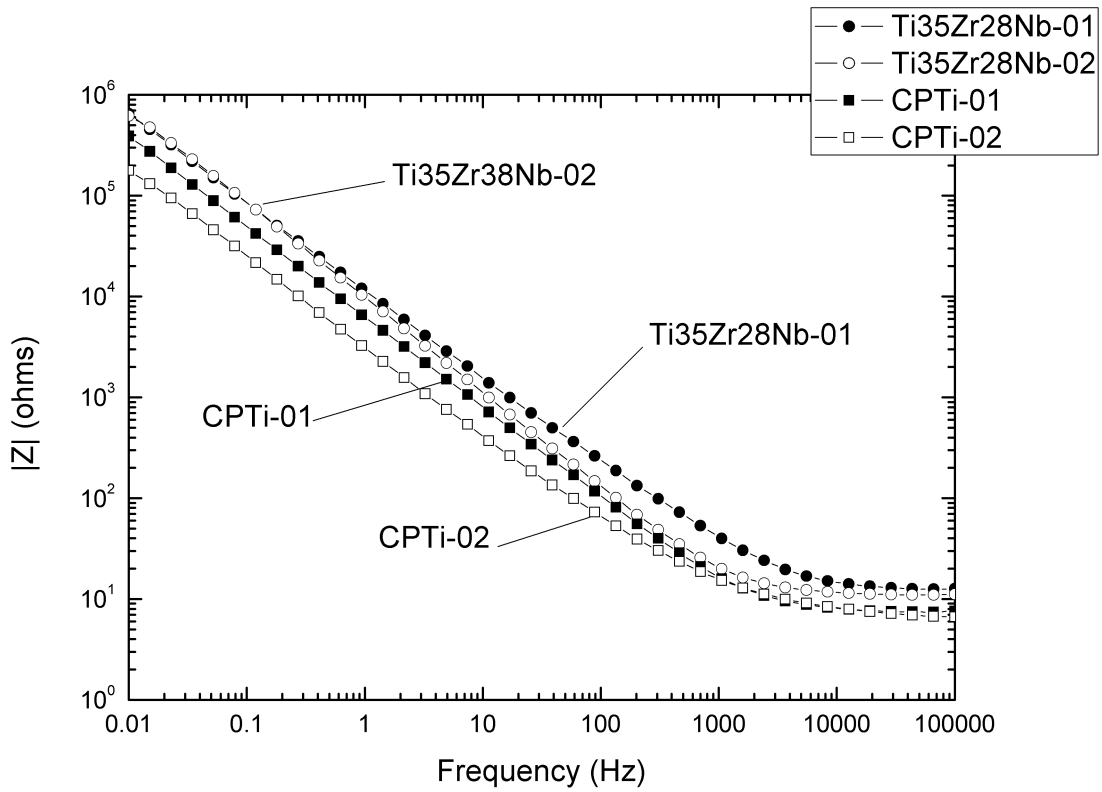

Figure 18: Bode plot comparison of all samples in 3.5% NaCl solution at 23 °C

Table 10: Characteristics of the Bode plot in 3.5% NaCl solution at 23 °C

Material	Sample	|Z| (kΩ)
CP Ti	1	390
	2	177
Ti alloy	1	651
	2	619

Figure 19 shows the phase angle approaching 90° for medium to low frequencies. This is seen for all samples in NaCl solution at 23 °C.

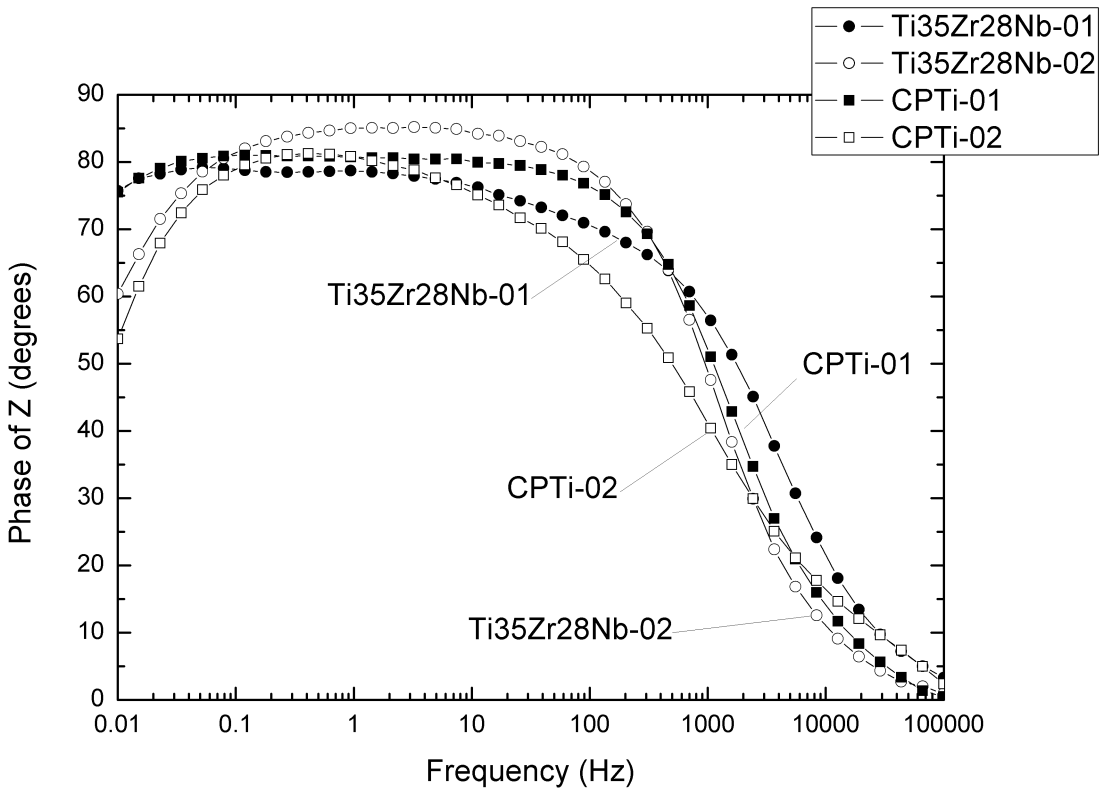

Figure 19: Phase plot comparison of all samples in 3.5% NaCl solution at 23 °C

Figure 20 shows the capacitance arcs of all samples in NaCl solution at 23 °C. The estimated arc diameters are shown Table 11.

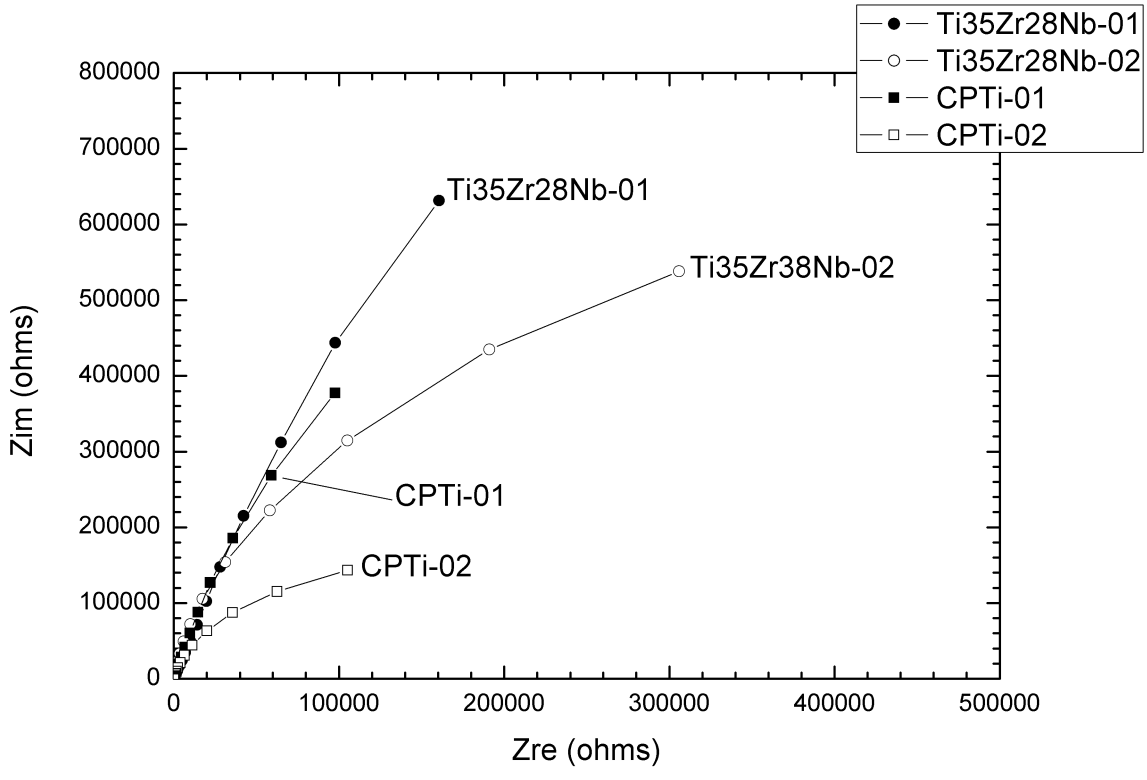

Figure 20: Nyquist plot comparison of all samples in 3.5% NaCl solution at 23 °C

Table 11: Characteristics of the Nyquist plot in 3.5% NaCl solution at 23 °C

Material	Sample	Diameter (kΩ)
CP Ti	1	3126
	2	366
Ti alloy	1	5956
	2	1554

4.3.4. Potentiodynamic Polarisation Curve

Potentiodynamic polarisation curves show corrosion potential versus current density (A/cm^2). The corrosion potential, passivation current density and film breakdown potential can be found from the polarisation curves.

4.3.4.1. Hanks' solution

Figure 21 compares the polarisation curves for all CP Ti and Ti alloy samples in Hanks' solution at 37 °C. The open circuit potential (OCP), film breakdown potential (E_b), passive current density (i_{pass}) and passive range (E_b – OCP) is shown in Table 12.

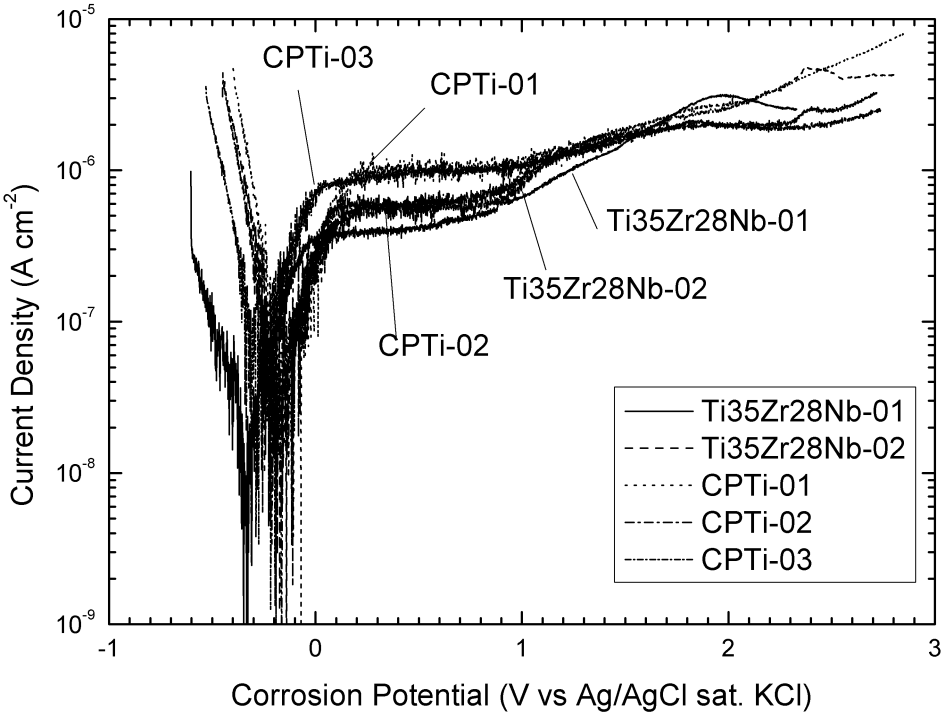

Figure 21: Polarisation curve comparison of all samples in Hanks' solution at 37 °C

It can be observed from the polarisation curve that the corrosion potential increased positively with the immersion time. The region of constant anodic current density with increasing corrosion potential represents the passivation process.

There is evidence of passive film breakdown when the anodic anodic current density increases suddenly after the E_b. There is also evidence of a re-passive state where the current density stabilises again.

Overall, the polarisation curves show very low i_{pass} values, in the order of 10^{-6} A/cm^2 (refer to Table 12).

Table 12: Characteristics of the polarisation curves in Hanks' solution at 37 °C

Material	Sample	OCP (mV)	E_b (mV)	i_{pass} (μA/cm^2)	Passive Range (mV)
CP Ti	1	-70	1020	1.02	1090
	2	-165	820	0.43	985
	3	-191	940	0.82	1131
Ti alloy	1	-327	480	0.77	807
	2	-141	860	1.30	1001

4.3.4.2. NaCl solution

Figure 22 compares the polarisation curves for all CP Ti and Ti alloy samples in 3.5% NaCl solution at room temperature (23 °C). The open circuit potential (OCP), film breakdown potential (E_b), passive current density (i_{pass}) and passive range (E_b – OCP) is shown in Table 13.

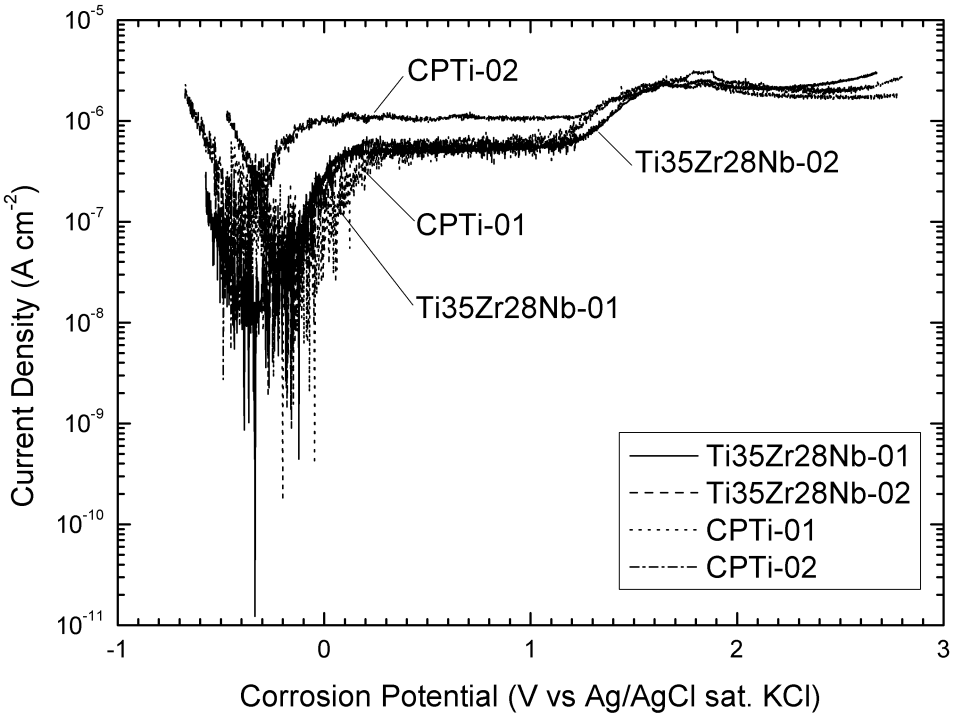

Figure 22: Polarisation curve comparison of all samples in 3.5% NaCl solution at 23 °C

Figure 22 shows the corrosion potential increased positively with the immersion time and the spontaneous formation of a protective film (as shown in Figure 21). There is also evidence of passive film breakdown and a re-passive state. It is noted that the film breakdown potential is higher in NaCl solution than Hanks' solution.

The polarisation curves show very low i_{pass} values, in the order of 10^{-6} A/cm^2 (see Table 13).

Table 13: Characteristics of the polarisation curves in 3.5% NaCl solution at 37 °C

Material	Sample	OCP (mV)	E_b (mV)	i_{pass} (μA/cm^2)	Passive Range (mV)
CP Ti	1	-201.2	1068	0.57	1269
	2	-488.7	1196	1.04	1685
Ti alloy	1	-334.8	1136	1.13	1471
	2	-157.6	1180	0.57	1338

5. Discussion

5.1.Immersion Testing

5.1.1. Surface Morphology

Surface morphology of CP Ti and Ti-35Zr-28Nb shows little changes to the surface. No evidence of pitting or crevice corrosion. Filiform corrosion was found on the surface of the CP Ti, however this is indicative of passive materials.

5.1.2. Weight Loss Measurements

The change in weight of the samples in both Hanks' solution and NaCl solution was in the order on 0.0001g. Therefore, the weight loss is considered negligible. This also indicates a low corrosion rate.

5.1.3. Surface Composition

Presence of calcium (Ca), phosphorus (P) and oxygen (O) suggests that the surface layer may be calcium phosphate, $Ca_{10}(PO_4)_6(OH)_2$ (also called hydroxyapatite). Calcium phosphate is a corrosion inhibitor, known to play a protective role for Ti and Ti alloys, resulting in a decrease in corrosion rate. The slight decrease in both Zr and Nb contents confirms a low corrosion rate.

5.1.4. Solution Analysis

Low concentration of Ti was detected in both solutions for CP Ti. Low concentration of Ti, Zr and Nb was detected in both solutions for the Ti alloy. It was noted that a higher concentration of Nb was found compared to Zr, despite having a lower content.

The concentration detected in the solutions was typically higher for the NaCl solution than Hanks' solution. This was expected as NaCl contains higher chloride content. It was also at an elevated temperature, further increasing corrosion rates.

Overall the low concentration of Ti, Zr, Nb detected was considered negligible indicating a low corrosion rate.

From the above discussion, it can be observed that the corrosion of CP

Ti and Ti alloy is a passivation process in both the Hanks' solution and 3.5% NaCl solution.

5.2.Electrochemical Testing

5.2.1. OCP

The trends shown in Figure 13 and Figure 14 indicate the spontaneous formation of a protective film on the surface of all samples. An increase in corrosion potential indicates thickening of the protective film. Overall, both CP Ti and Ti35Zr28Nb exhibit passivation behaviour in Hanks' solution and NaCl solution. Passivation behaviour is indicative of low corrosion rates.

5.2.2. EIS

High modulus of impedance (Z) at low frequencies is seen for all samples in both Hanks' solution and NaCl solution. This indicates high polarisation resistance and consequently low corrosion rate.

The phase plots show the phase angle approach 90° for medium to low frequencies. This indicates a highly capacitive behaviour of all samples in Hanks' solution and NaCl solution. This is typical of passive materials, suggesting that a highly stable film was formed on all tested samples.

A wide capacitance arc indicates an increase in reaction resistance. This indicates a dense passive film is formed on the surface. This is seen in all samples in Hanks' solution and NaCl, indicating a low corrosion rate.

5.2.3. Potentiodynamic Polarisation Curve

The nature of the polarisation curves indicate that all samples exhibit self-passivation behaviour. Partial stabilisation of current density suggests that a protective passive film is formed within the potential range.

At approximately 1V the passive film is seen to breakdown in all samples. This is caused by the chloride ions from the solution. The restoration time for the passive film is shorter for CP Ti, suggesting it has a more stable and protective film.

The polarisation curves show very low I_{corr} values (in the order of 10^{-6} A/cm^2). This is typical of passive materials. Overall, the passivation behaviour of both the materials indicate low corrosion rates.

5.3.Experimental Difficulties

Throughout the experimental procedure, there were several difficulties, which could have potentially affected the results, including but not limited to:

- Potential inconsistencies in sample preparation: The samples were unable to be automatically ground and polished using Struers Tegraforce-5 orbital machine due to nature of the corrosion testing. The samples were unable to be mounted due to the coupon assembly configuration. Therefore, it was restricted to manual surface preparation only. This made it difficult to ensure the surface preparation was consistent for all samples.
- Scratches during polishing: There were suspected diamond particles embedded in the polishing cloth from previous usage where diamond paste was used for polishing. This resulted in faint scratches on the sample surface during the final polishing step.
- Inconsistencies in coupon assembly: Due to the small and slightly varied sizes of the samples it was difficult to perfectly align the stack of PTFE washers and samples. This may have resulted in a difference in crevice simulation between samples.
- Evaporation of the water bath: Over the 28 days of testing the water bath experienced some water evaporation, requiring the water bath to be topped up to the required water level. This resulted in minor disturbances to the water bath temperature.
- Evaporation during immersion testing: Over the duration of the immersion testing the beaker/flask experienced evaporation. This may have affected the concentration of the solution. Steps were taken to minimise these effects, including covering the beaker and the use of a cooling system.

- Cleaning samples: Before the samples were weighed, they were cleaned using a solution of nitric acid (HNO_3) and hydrofluoric acid (HFl). This may have influenced the corrosion. However, the overall weight loss was considered negligible.

6. Conclusion

The experimental investigation of corrosion stability of Ti-35.4Zr-28Nb in synthetic body fluid was conducted to aid in the development of a porous Ti alloy for use as a bone replacement material. The corrosion analysis was conducted using immersion testing, OCP, EIS and potentiodynamic polarisation curves

Based on the experimental results and corrosion analysis, no significant evidence of crevice corrosion was observed under the testing conditions indicating that both CP Ti and the Ti alloy are not sensitive to crevice corrosion. This conclusion of low corrosion rate was made based on the following observations:

- Low weight loss and low concentration of Ti, Zr and Nb found after immersion testing
- Corrosion potential increases and stabilises during OCP measurement indicating a typical passivation behaviour
- High modulus of impedance (Z) at low frequencies, indicating high polarisation resistance
- Phase angle close to 90° for medium to low frequencies, indicating a highly capacitive behaviour
- A wide capacitance arc, indicating passive film formation
- Polarisation curves show partial stabilisation of current density and overall low current densities (in the order of 10^{-6} A/cm^2), indicating passivation behaviour.

Further tests could be conducted using an increased immersion time (>28 days) in Hanks' solution at 37 °C to understand the long-term effects. Further research could also investigate the effects of porosity on the corrosion stability of Ti-35.4Zr-28Nb.

7. References

ASSIS, S. L. D., WOLYNEC, S. & COSTA, I. 2006. Corrosion characterization of titanium alloys by electrochemical techniques. *Electrochimica Acta,* 51**,** 1815-1819.

BANSIDDHI, A. & DUNAND, D. C. 2014. *Titanium and NiTi foams for bone replacement.*

BINYAMIN, G., SHAFI, B. M. & MERY, C. M. 2006. Biomaterials: A primer for surgeons. *Seminars in Pediatric Surgery,* 15**,** 276-283.

BIRLA, R. 2014. Biomaterials for Tissue Engineering. *Introduction to Tissue Engineering.* John Wiley & Sons, Inc.

CHENG, F. T., LO, K. H. & MAN, H. C. 2007. An electrochemical study of the crevice corrosion resistance of NiTi in Hanks' solution. *Journal of Alloys and Compounds,* 437**,** 322-328.

CHENGHAO, L., LI, AMP, APOS, NAN, J., CHUANJUN, Y. & NAIBAO, H. 2015. Crevice Corrosion Behavior of CP Ti, Ti-6Al-4V Alloy and Ti-Ni Shape Memory Alloy in Artificial Body Fluids. *Rare Metal Materials and Engineering,* 44**,** 781-785.

CRAMER, S. D., COVINO, B. S. & COMMITTEE, A. I. H. 2003. *Corrosion: Fundamentals, Testing and Protection*, ASM International.

CREMASCO, A., OSÓRIO, W. R., FREIRE, C. M. A., GARCIA, A. & CARAM, R. 2008. Electrochemical corrosion behavior of a Ti–35Nb alloy for medical prostheses. *Electrochimica Acta,* 53**,** 4867-4874.

DAVIS, J. 2003. Overview of biomaterials and their use in medical devices. *Handbook of materials for medical devices. Illustrated edition, Ohio: ASM International***,** 1-11.

FOJT, J., JOSKA, L. & MÁLEK, J. 2013. Corrosion behaviour of porous Ti–39Nb alloy for biomedical applications. *Corrosion Science,* 71**,** 78-83.

JONES, D. A. 1996. *Principles and prevention of corrosion / Denny A. Jones,* Upper Saddle River, NJ, Upper Saddle River, NJ : Prentice Hall.

LOPES, É., SALVADOR, C., ANDRADE, D., CREMASCO, A., CAMPO, K. & CARAM, R. 2016. Microstructure, Mechanical Properties, and Electrochemical Behavior of Ti-Nb-Fe Alloys Applied as Biomaterials. *Metallurgical and Materials Transactions A,* 47**,** 3213-3226.

MARTINS, D. Q., OSÓRIO, W. R., SOUZA, M. E. P., CARAM, R. & GARCIA, A. 2008. Effects of Zr content on microstructure and corrosion resistance of Ti–30Nb–Zr casting alloys for biomedical applications. *Electrochimica Acta,* 53**,** 2809-2817.

NIEMEYER, T. C., GRANDINI, C. R., PINTO, L. M. C., ANGELO, A. C. D. & SCHNEIDER, S. G. 2009. Corrosion behavior of Ti–13Nb–13Zr alloy used as a biomaterial. *Journal of Alloys and Compounds,* 476**,** 172-175.

NNAMCHI, P. S., OBAYI, C. S., TODD, I. & RAINFORTH, M. W. 2016. Mechanical and electrochemical characterisation of new Ti–Mo–Nb–Zr alloys for biomedical applications. *Journal of the Mechanical Behavior of Biomedical Materials,* 60**,** 68-77.

OZAN, S., LIN, J., LI, Y., IPEK, R. & WEN, C. 2015. Development of Ti–Nb–Zr alloys with high elastic admissible strain for temporary orthopedic devices. *Acta Biomaterialia,* 20**,** 176-187.

TEMENOFF, J. S. & MIKOS, A. G. 2008. *Biomaterials : the intersection of biology and materials science / J. S. Temenoff, A.G. Mikos,* Upper Saddle River, N.J., Upper Saddle River, N.J. : Pearson/Prentice Hall.

WATANABE, Y., SATO, H. & MIURA-FUJIWARA, E. 2015. Functionally Graded Metallic Biomaterials. *In:* NIINOMI, M., NARUSHIMA, T. & NAKAI, M. (eds.) *Advances in Metallic Biomaterials: Processing and Applications.* Berlin, Heidelberg: Springer Berlin Heidelberg.

XU, Y.-F., XIAO, Y.-F., YI, D.-Q., LIU, H.-Q., WU, L. & WEN, J. 2015. Corrosion behavior of Ti–Nb–Ta–Zr–Fe alloy for biomedical applications in Ringer's solution. *Transactions of Nonferrous Metals Society of China,* 25**,** 2556-2563.

ZAINAL ABIDIN, N. I., ATRENS, A. D., MARTIN, D. & ATRENS, A. 2011. Corrosion of high purity Mg, Mg2Zn0.2Mn, ZE41 and AZ91 in Hank's solution at 37 °C. *Corrosion Science,* 53**,** 3542-3556.

8. Appendices

8.1. Appendix A

HANKS' BALANCED SALTS [HBSS]
Without Sodium Bicarbonate and Phenol Red
Product Number **H1387**

Product Description
Although there have been many modifications to the original formulas in efforts to produce fully defined media, salt solutions still play an important role in tissue culture. A salt solution's basic function, to maintain the pH and osmotic balance in the medium and to provide the cells with water and essential inorganic ions, is as valuable today as when it was first developed a century ago.

Components	g/L
Calcium Chloride (anhydrous)	0.1396
Magnesium Sulfate(anhydrous)	0.09767
Potassium Chloride	0.4
Potassium Phosphate Monobasic (anhydrous)	0.06
Sodium Chloride	8.0
Sodium Phosphate Dibasic (anhydrous)	0.04788
D-Glucose	1.0

Precautions and Disclaimer
REAGENT
For R&D use only. Not for drug, household or other uses.

Preparation Instructions
Powdered salts are hygroscopic and should be protected from moisture. The entire contents of each package should be used immediately after opening. Preparing a concentrated salt solution is not recommended as precipitates may form. Supplements can be added prior to filtration or introduced aseptically to sterile salt solution.

1. Measure out 90% of final required volume of water. Water temperature should be 15-20 °C.
2. While gently stirring the water, add the powdered medium. Stir until dissolved. Do NOT heat.
3. Rinse original package with a small amount of water to remove all traces of powder. Add to solution in step 2.
4. To the solution in step 3, add 0.35 g sodium bicarbonate or 4.7 ml of sodium bicarbonate solution [7.5%w/v] for each liter of final volume of medium being prepared. Stir until dissolved.
5. While stirring, adjust the pH of the medium to 0.1-0.3 pH units below the desired pH since it may rise during filtration. The use of 1N HCl or 1N NaOH is recommended.
6. Add additional water to bring the solution to final volume.
7. Sterilize immediately by filtration using a membrane with a porosity of 0.22 microns.
8. Aseptically dispense medium into sterile container.

Storage and Stability
Store the dry powdered salts at 2-8 °C under dry conditions and liquid medium at 2-8 °C in the dark. Deterioration of the powdered medium may be recognized by any or all of the following: [1] color change, [2] granulation/clumping, [3] insolubility. Deterioration of the liquid medium may be recognized by any or all of the following: [1] pH change, [2] precipitate or particulates, [3] cloudy appearance [4] color change. The nature of supplements added may affect storage conditions and shelf life of the medium. Product label bears expiration date.

Procedure
Materials Required but Not Provided
Water for tissue culture use [W3500]
Sodium Bicarbonate [S5761] or
Sodium Bicarbonate Solution, 7.5% [S8761]
1N Hydrochloric Acid [H9892]
1N Sodium Hydroxide [S2770]
Medium additives as required

References
1. Hanks, J. (1976) Hanks' Balanced Salt Solution and pH Control. Tissue Culture Association Manual. 3, 3.

Revised: April 2007